Cell Search Procedures in LTE Systems

Vikas Paliwal, Ioannis Lambadaris
Department of Systems and Computer Engineering
Carleton University, Ottawa, ON, Canada, K1S 5B6
{vpaliwal, ioannis}@sce.carleton.ca

***Abstract*—In this paper, we present a cell search procedure for a Long Term Evolution (LTE) system based device, which involves determining the primary group identifier associated with a cell as well as its timing information. This is facilitated by using the primary synchronization signal available in an LTE system. For the first stage of cell search, this paper presents a time-domain based cell search procedure in an LTE system. Further, we evaluate the performance of such an approach with varying levels of noise and present the design considerations to be utilized in developing a searcher hardware block. We also present analytical and simulation results to evaluate the searcher performance.**

***Index Terms*—Cell Search, LTE, Zadoff-Chu Sequences, Synchronization.**

I. Introduction

CELL search procedures are the first set of tasks performed by a mobile device in a cellular system after initial power-up. It is only after the search and registration procedures, a mobile device is able to receive and initiate voice and data calls. A typical cell search procedure in cellular systems such as third-generation partnership project's (3GPP) - Long Term Evolution (LTE), Wideband Code Division Multiple Access (WCDMA) or Global System for Mobile Communications (GSM) - may involve a combination of carrier frequency determination, timing synchronization and identification of unique cell identifier. These procedures are typically facilitated by specific synchronization signals transmitted by the base station (BTS). However, these synchronization signals are not continuously used in connected modes for a mobile device. Hence, only minimum resources in terms of power, subcarrier allocation and time slice are allocated for synchronization signals.

In an LTE system, a Zadoff-Chu sequence [6], which has good auto-correlation properties in frequency domain, is used to generate samples for the primary synchronization signal (PSS). Further, these autocorrelation properties are preserved in the time domain as well. Consequently, matched filter based time-domain autocorrelation approaches are applicable to PSS as well. However, the sampling rate for correlation (as in [11]) needs to be carefully chosen to avoid excessive processing and yet maintain a good level of cell detectability in cell search procedures. Further, it needs to be understood as to how the correlation scheme behaves in the presence of extraneous noise. It is therefore essential to analyze the impact of these factors on the performance of cell search procedure in LTE systems. It is important to mention that the first stage of cell search process involving the PSS channel is most crucial

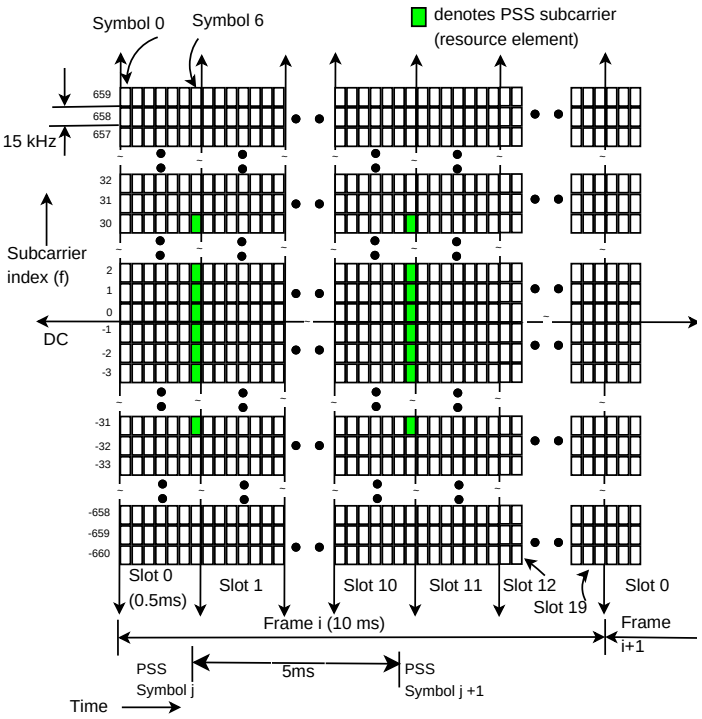

Fig. 1. Subcarrier and time-slice allocation for PSS with system bandwidth of 20MHz and 1320 subcarriers

in eventual successful detection of an LTE cell as has been reported in [5].

Complete details on LTE system and synchronization signal can be found in the reference texts [1] and the technical specifications [3]. Previous works on cell search procedures for 3GPP-LTE provide good detail on the system architecture and design choices. A good reference on design considerations for synchronization techniques for LTE can be found in [4]. More specifically, design ideas and performance results for cell search in LTE have been presented in [8] and [9]. Also, in [10], the initial cell search procedure has been combined with frequency error correction. Further, the work in [7] proposes to replace the existing synchronization sequence in LTE with an enhanced perfect sequence. However, existing research literature does not fully address the relation of a key performance metric, cell detectability, with system design parameters and noise levels. This paper attempts to analyze the performance of cell search procedure in LTE system by means of analysis and simulations. More specifically, the challenges that are present in a cellular wireless communication due to system noise are

analyzed against the cell search parameters such as sampling rate and accumulation length. The analysis and methods proposed here can be applied to meet the contending demands of successful cell detection and minimal processing complexity. In the following section, we begin with a discussion of LTE system's primary synchronization signal (PSS). Then in section III, we cover the various design considerations for searcher block viz. sampling rate, filtering and non-coherent integration. This is followed by a proposed searcher hardware block architecture for PSS detection in section IV. We present a comparison of analytical and simulation results in section V. Finally we conclude with our future directions for research in section VI.

II. Primary Synchronization Signal

The LTE wireless cellular system is designed with orthogonal frequency domain multiple access (OFDMA) in the physical layer. The incoming user data bits are multiplexed onto the assigned sub-carriers in frequency domain and transmitted as a single time-domain signal in downlink. This is accomplished by an inverse fast fourier transform (IFFT) on the user data bits. For facilitating cell search procedures, known bit patterns are transmitted in specific time and frequency slots (also known as resource elements) for the mobile devices to be able to identify the cell's timing and its associated identifier (cell ID).

A mobile device after being powered on, attempts to measure the wideband received power for specific frequencies over a set of frequency bands. After ranking the frequencies based on received signal strength indicator (RSSI), the user equipment (UE) attempts cell search using the downlink synchronization channels. The cell search procedure in LTE system can be performed in three steps. The first step is carried out by correlating the received Primary Synchronization Signal (PSS) samples to determine the cell's group identity out of three possible values and its timing information by determining the 5ms (Figure 1) boundary of cell's signal transmission. The latter is due to the fact that PSS signal is transmitted as the last symbol in 0^{th} and 10^{th} slots of a 10ms frame. This can be followed by correlating the received samples of the secondary synchronization signal and reference signal [3] to determine the cell identifier and frame timing.

The PSS is composed of 62 samples of Zadoff-Chu sequence in the frequency domain that occupy the central sub-carriers in the transmission bandwidth as shown in Figure 1. The sequence that is used for frequency domain PSS samples in LTE is,

$$P_r(f) = \begin{cases} e^{-j\frac{\pi r(f+31)(f+32)}{63}} & f = -31, -30, \ldots, -1 \\ e^{-j\frac{\pi r(f+32)(f+33)}{63}} & f = 0, 1, \ldots, 30 \end{cases} \quad (1)$$

where r is the root of Zadoff-Chu sequence with three possible values of 25,29 and 34 and $P_r(f)$ forms the frequency domain sample sequence for PSS. As such the frequency domain samples in equation 1 exhibits very low autocorrelation for non-zero lag values. But frequency domain correlation is not practical as it requires determining the exact timing of the signal to perform the FFT operation and as such applying FFT on a large number of timing hypotheses is not practical.

TABLE I
Low pass filter coefficients

i	0	1	2	3	4	5	6
b[i]	0.09	-0.53	1.33	-1.76	1.33	-0.5381	0.091
a[i]	1	-5.8	13.82	-17.75	12.82	-4.95	0.79

TABLE II
Metrics with various downsampling rates

Downsampling Rate	1	2	4	8	16
Timing Hypotheses	153600	76800	38400	19200	9600
System SNR[1]	33 dB	30 dB	27 dB	24 dB	21 dB

III. Searcher Design

A. Sampling and Filtering Issues

As has been mentioned before, the Primary Synchronization Signal (PSS) occupies a bandwidth of 62 15kHz-subcarriers around the DC (Figure 1). Therefore, the low-pass filter to be used for extracting PSS signal from a larger spectrum should have a cutoff bandwidth corresponding to this. As a design example, for sampling rate of 30.72 Msps, the Nyquist frequency would be 15.36 MHz and bandwidth of low-pass filter needs to be 3 percent ($\frac{31 \cdot 0.015}{15.36} = 0.03$) of Nyquist frequency. Additionally it would be desirable to have a flat response in passband and a very sharp transition in gain between passband and stopband. These goals can be achieved by 5-th or 6-th order elliptic filters. An example of such a filter used in our simulations is shown in Table I, where $b[i]$s and $a[i]$s are respectively the numerators and denominators of filter's transfer function designed in MATLAB [14] using standard IIR filter design techniques [2]. In terms of correlation of time domain samples with PSS sequence, several sampling rates can be utilized with varying levels of system SNRs. The key criteria in choosing a good sampling rate are the contrasting demands of: (a) better accuracy attained at higher sampling rates and, (b) minimal gate count in ASIC implementation achieved by attempting fewer timing hypotheses with lower sampling rates. Based on these trade-offs, for a PSS based synchronization implementation, the cell search process can be split into two parts - a coarse search that performs PSS correlation at the minimum possible rate, e.g. the incoming samples at 30.72 MHz are down-sampled at $\frac{1}{16}$ rate so that Nyquist frequency ($\frac{30.72}{16 \cdot 2}$ = 0.96 MHz) is greater than PSS bandwidth ($62 \cdot 15$ kHz= 0.93MHz). It can be followed by a far more accurate fine search with maximum allowed incoming sampling rate (e.g. 30.72 MHz). This ensures that the coarse search yields the approximate location of PSS peaks across multiple timing hypotheses with minimal hardware complexity. This is followed by a significantly shortened window of fine search around the results from coarse search so that exact signal level can be estimated for other purposes e.g. crystal frequency correction. Table II shows the number of possible timing hypotheses to be tried for various sampling rates and the corresponding System SNR degradation as explained in section III-C[1].

[1]System SNR as derived later in section III-C

B. Time Domain Analysis

The frequency domain auto-correlation properties of Zadoff-Chu sequence are applicable to time domain as well. By ignoring the small anomalous spikes for non-zero lag values when performing the frequency domain autocorrelation of Zadoff-Chu sequence, its auto-correlation behavior can be directly computed and approximated by,

$$R(\nu) = \sum_{f=-31}^{f=30} P_r(f) \cdot P_r^*(f+\nu) = \begin{cases} 62 & \nu = 0 \\ 0 & \nu \neq 0 \end{cases} \quad (2)$$

This approximation can be extended in time domain by recognizing that an inverse discrete fourier transform of a constant amplitude zero autocorrelation waveform such as in eqn. 2 preserves the property of out-of-phase autocorrelation being equal to zero. This can be understood by assuming only the 62 subcarriers used by PSS are occupied and realizing that an M-point IDFT is a linear combination of the following form,

$$p_r[n] = \sum_{f=-\frac{M}{2}}^{f=\frac{M}{2}-1} P_r(f) * e^{\frac{j2\pi fn}{M}} = \sum_{f=-31}^{f=30} P_r(f) * e^{\frac{j2\pi fn}{M}} \quad (3)$$

As in [6], the IDFT matrix for time-shift τ is defined as, $\mathbf{F}(\tau) = \begin{bmatrix} F[\tau, -\frac{M}{2}] & \cdot & \cdot & \cdot & F[\tau, \frac{M}{2}-1] \\ \cdot & \cdot & \cdot & \cdot & \cdot \\ F[k+\tau, -\frac{M}{2}] & \cdot & F[k+\tau, f] & \cdot & F[k+\tau, \frac{M}{2}-1] \\ \cdot & \cdot & \cdot & \cdot & \cdot \\ F[M-1+\tau, -\frac{M}{2}] & \cdot & \cdot & \cdot & F[M-1+\tau, \frac{M}{2}-1] \end{bmatrix}$

where $F[a,b] = e^{\frac{j2\pi ab}{M}}$. The Zadoff-Chu sample matrix can be represented as, $\mathbf{P_r} = [0 \ldots 0 \quad P_r[-31] \ldots P_r[f] \ldots P_r[30] \quad 0 \ldots 0]$ (total M frequency components with zero samples beyond PSS bandwidth, refer Fig. 1). Hence, the time-domain sample matrix corresponding to this is, $\mathbf{p_r} = \mathbf{P_r} \cdot \mathbf{F(0)}$. Based on these, the time-domain autocorrelation can be derived in matrix form as:

$$R(\tau) = \sum_{k=0}^{M-1} p_r[k] \cdot p_r^*[k+\tau] = \mathbf{P_r} \cdot \mathbf{F(0)} \cdot \mathbf{F}(\tau)^* \cdot \mathbf{P_r^*} =$$

$$\mathbf{P_r} \cdot \begin{bmatrix} 0 & 0 & \cdot & M & 0 & \cdot & 0 \\ 0 & 0 & \cdot & 0 & M & \cdot & 0 \\ \cdot & \cdot & \cdot & \cdot & \cdot & \cdot & \cdot \\ M & 0 & \cdot & 0 & 0 & \cdot & 0 \\ 0 & M & \cdot & 0 & 0 & \cdot & 0 \\ \cdot & \cdot & \cdot & \cdot & \cdot & \cdot & \cdot \\ 0 & 0 & \cdot & 0 & 0 & \cdot & 0 \end{bmatrix} \cdot \mathbf{P_r^*} = M\mathbf{P_r}\mathbf{I}(0,\tau)\mathbf{P_r^*}$$

$$\Rightarrow R(\tau) = \begin{cases} 62 \cdot M & \tau = 0 \\ 0 & \tau \neq 0 \end{cases} \quad (4)$$

where $\mathbf{I}(a,b)$ denotes identity matrix shifted by a rows and b columns. Simulation results for the time domain behavior is shown in Figure 2. This indicates PSS has good autocorrelation properties in time domain as well. Even though frequency domain PSS sequence has good autocorrelation properties, it requires fairly large number of FFT operations to be performed on multiple timing hypotheses requiring complex ASIC implementation with increased power requirements. On the other hand, time-domain correlation has good autocorrelation properties and can be easily accomplished by simple correlation with time-domain PSS sequence with reduced complexity and resources.

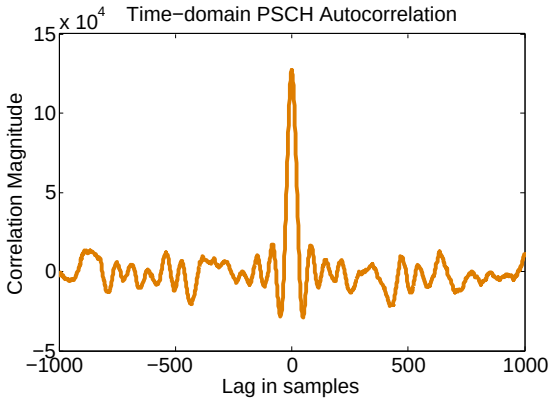

Fig. 2. Time domain correlation behavior of PSS

C. System SNR

In an OFDMA system like LTE, the data on individual subcarriers remains orthogonal in frequency domain to PSS symbols (i.e. after performing the FFT operation). But, when correlation of PSS sequence is done with incoming samples in time-domain, the data subcarriers appear as source of randomized noise for PSS synchronization. The 3GPP LTE specifications mandate transmission bandwidths from 1.4 MHz to 20 MHz, with number of 15 kHz subcarriers (N_s) ranging from 72 to 1320 (Figure 1). In order to mitigate the impacts of noise contribution from higher subcarriers, a LTE UE for time-domain PSS correlation may employ a discrete low-pass filter that rejects all frequencies beyond the bandwidth of PSS signal, ie. equivalent to 62 subcarriers (62×15kHz = 93kHz) centered around the DC center point.

The data bits are modulated using one of the modulation schemes (QPSK, 16QAM, 64QAM etc) and essentially correspond to mapping a set of bits to one of the complex modulation symbols. As an example, for a random stream of incoming data bits (guaranteed by bit scrambling), the symbol for QPSK modulation could be uniformly distributed over the following set: $\{\pm\frac{1}{\sqrt{2}} \pm \frac{1}{\sqrt{2}}j\}$. It is therefore reasonable to consider data bits as i.i.d. and uniformly distributed over these values with zero mean and unity variance. Other modulation schemes could be modeled in a similar manner.

In time domain, a perfectly aligned PSS sequence has the autocorrelation properties in eqn.4, but the wrong timing hypotheses would take a number of M_1 samples from one OFDM symbol and the remaining M_2 samples from the next ($M_1 + M_2 = M$). This translates to time-domain samples $\{d[M-M_1], d_[M-M_1+1], \ldots d_[M-1]\}$ formed by IDFT of data symbols $\{D(-\frac{N_s}{2}), D(-\frac{N_s}{2}+1), \ldots, D(\frac{N_s}{2}-1)\}$ and $\{d^{'}[1], d^{'}[2], \ldots d^{'}[M_2]\}$ formed by IDFT of data symbols $\{D^{'}(-\frac{N_s}{2}), D^{'}(-\frac{N_s}{2}+1), \ldots, D^{'}(\frac{N_s}{2}-1)\}$. Assuming a perfect low-pass filter, only 62 subcarriers (i.e. $\{D(-31), D(-30), \ldots, D(30)\}$ and

$\{D^{'}(-31), D^{'}(-30), \ldots, D^{'}(30)\}$) corresponding to PSS will contribute to inherent system noise as higher subcarriers will be filtered out. This would be correlated by the time domain PSS sequence, $p_r[n]$, as shown in equation 3. Therefore, the time domain correlation corresponding to timing hypothesis M_1 would be,

$$C(M_1) = \sum_{n=M-M_1}^{M-1} p_r^*[n-M+M_1] \cdot d[n] + \sum_{n=0}^{M_2-1} p_r^*[n+M_1] \cdot d^{'}[n] \tag{5}$$

Due to low-pass filtering upto PSS bandwidth, this translates to,

$$C(M_1) = \sum_{f=-31}^{30} D(f) \{ \sum_{n=M-M_1}^{M-1} p_r^*[n-M+M_1] \cdot e^{\frac{j2\pi fn}{M}} \} + \sum_{f=-31}^{30} D^{'}(f) \{ \sum_{n=0}^{M_2-1} p_r^*[n+M_1] \cdot e^{\frac{j2\pi fn}{M}} \} \tag{6}$$

As mentioned before, the data symbols $D(f)$ and $D^{'}(f)$ can be thought of complex random variables with zero mean and unity variance. Also, due to good non-periodic polyphase correlation properties of Zadoff-Chu sequence and the fact that each of term $p_r^*[n - M + M_1] * e^{\frac{j2\pi fn}{M}}$ is a linear combination of original Zadoff-Chu sequence and therefore is also a perfect sequence. As a result, each of multiplicands of $D(f)$ and $D^{'}(f)$ can be approximated with a squared magnitude contributed by auto-correlation of $p_r(n)$ with itself only. Therefore, correlation corresponding to hypothesis, $C(M_1)$, as a linear combination of 62 random variables, is distributed like:

$$\begin{aligned} C(M_1) &\sim \mathbf{N}(0, 62 \cdot (\sum_{n=0}^{M_1-1} p_r^*[n] \cdot p_r[n] + \sum_{n=M_1}^{M-1} p_r^*[n] \cdot p_r[n])) \\ &\sim \mathbf{N}(0, 62 \cdot (62 \cdot M)) \end{aligned} \tag{7}$$

The last result is possible due to autocorrelation of time-domain PSS as derived in equation 4. As a consequence of these two results, the system SNR obtained by squaring the I/Q components for signal and noise hypotheses can be estimated as, $SNR = \frac{(62 \cdot M)^2}{62 \cdot 62 \cdot M} = M$. Therefore, assuming no other noise sources, the overall system SNR for PSS signal against a noise hypothesis is $10log_{10}M$, or +33 dB for a sampling/correlation rate of 30.72 Msps.

D. SNR with AWGN noise

Apart from inherent system noise, the LTE channel has noise contributions from other sources viz. thermal noise, leakage noise from neighboring cells, other radio access technologies (RATs) etc. All these noise sources can generally be modeled as additive white gaussian noise (AWGN) [3]. Due to the low-pass filtering employed with PSS based synchronization, the impact of additive noise is accumulated only over $+/-31$ subcarriers around DC. Referring to equation 2, each of the frequency domain samples can be thought of as composed of PSS contribution and AWGN component. As a result, the frequency domain samples $D(f)$ is a sum of the form, $D_s(f) + N_s(f)$, where $D_s(f)$ is the data sample on the specific radio resource element (RE) with zero mean and variance equal to I_{or} mean power spectral density (PSD) of transmitted signal averaged over RE (defined in [3], TS 36.521). The noise samples $N_s(f)$ also have zero mean but variance being N_{oc} ie. the PSD of white noise per RE [3]. This indicates at the noise hypothesis, $C(M_1)$ as in eqn. 6, distributed as: $C(M_1) \sim \mathbf{N}(0, 62 \cdot (62 \cdot M))$, which when combined with eqns. 5 and 7, yields to the effective SNR relation as:

$$\text{SNR}_{AWGN} = \frac{M \cdot I_{or}}{I_{or} + N_{oc}} \tag{8}$$

E. Cell Detection Probability under Non-coherent Combining

Non-coherent combining refers to accumulation of magnitudes of correlated complex symbols while discarding the phase components in doing the accumulation. Compared to a coherent combining scheme that correlates and accumulates each of the contiguous time-doman samples while preserving the complex phasors, non-coherent combining is very useful in a situation where the symbols to be accumulated are spread wide apart in time and hence coherent combination is not reliable. This is due to the phase shifts caused by factors such as mobility of the wireless device or inherent frequency errors in the crystal oscillators utilized for providing the timing reference. Clearly, longer non-coherent accumulation enhances the effective SNR of the PSS signal. More specifically, after accumulating the primary synchronization signal over p slots in a non-coherent manner the correlation metric turns out as a squared sum of p normal random variables distributed according to equation 7. The signal hypothesis for such non-coherent accumulation grows linearly as $C_S = p \cdot (62 \cdot M)^2$. As such, the squared sums of the noise correlation corresponding to timing hypothesis M_1, is distributed as a chi-square distribution with $2p$ degrees of freedom, with a factor of two for I/Q branches.

$$C_N(M_1) = \sum_{k=0}^{p-1} C^2(M_1, k) \sim \chi^2_{2p}(0, (I_{or} + N_{oc}) \cdot 62 \cdot (62 \cdot M)) \tag{9}$$

Based on these results and those in previous sections, we are now in a position to derive the expression for probability of detection of cell at primary synchronization stage. By normalizing the AWGN noise to have unity power, the signal power can be derived from equation 8. We can denote it as snr. Essentially a PSS signal hypothesis corresponding to correct timing has a signal($R(\tau)$) and noise($C_N(M_1)$) components as described in equations 4 and 9. Thus signal hypothesis corresponding to correct timing, has a real component distributed as $\mathbf{N}(\sqrt{snr}, \frac{1}{2})$ and imaginary component as $\mathbf{N}(0, \frac{1}{2})$. The I/Q accumulations could potentially have been rotated by channel fading, so a squared magnitude is necessary which will follow a non-central chi-square distribution of degree 2 with non-centrality parameter $\lambda = (\frac{\mu_1}{\sigma_1})^2 + (\frac{\mu_2}{\sigma_2})^2 = 2 \cdot snr$. After p symbols of non-coherent combining, this translates to non-central chi-square distribution of degree $2p$ and non-centrality parameter $\lambda = 2 \cdot p \cdot snr$, distributed according to $f_s(x) = \frac{1}{2} e^{-\frac{(x+\lambda)}{2}} (\frac{x}{\lambda})^{\frac{p}{2} - \frac{1}{2}} I_{p-1}(\sqrt{\lambda x})$, where $I()$ is modified Bessel function of first kind. The noise timing hypotheses

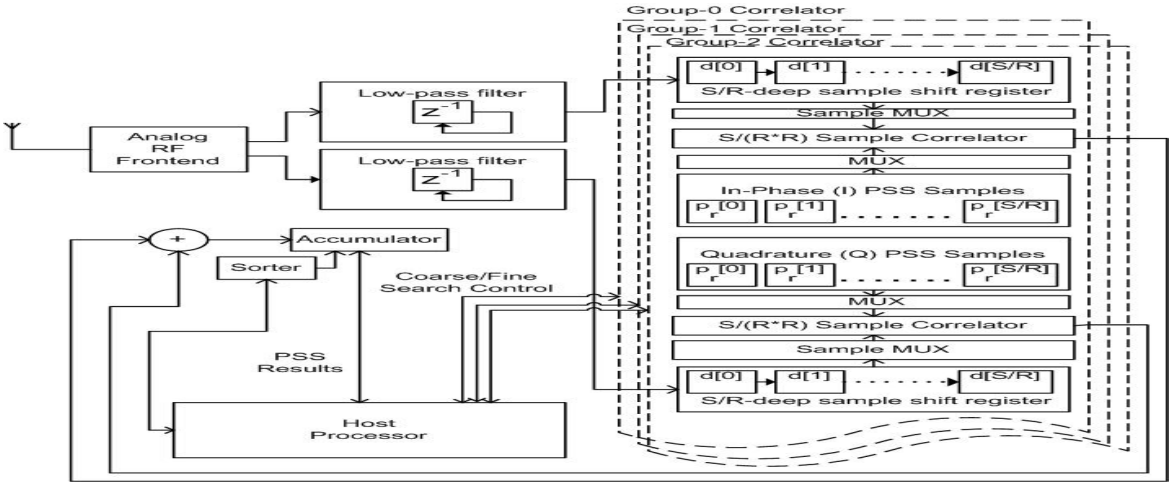

Fig. 3. Architecture for primary synchronization

based on eqn. 9, and normalization to unity, remain as central chi-square distribution(CDF, $F_n(x) = \frac{\gamma(p,x/2)}{\Gamma(p)}$) of degree $2p$ composed of normally distributed random variables with mean zero and variance $\frac{1}{2}$. The number η of such noise hypotheses is determined by table II. For a successful detection the maximum of all of these η noise hypotheses needs to be less than signal hypothesis. The maximum of these η noise hypotheses is distributed according to $F_{max,n}(x) = (F_n(x))^\eta$. Thus the successful cell search detection probability can be determined as,

$$P_d(snr, p, \eta) = \int_0^\infty f_s(x) F_{max,n}(x) \cdot dx$$

$$= \int_0^\infty \frac{1}{2} e^{-\frac{(x+\lambda)}{2}} (\frac{x}{\lambda})^{\frac{p}{2}-\frac{1}{2}} I_{p-1}(\sqrt{\lambda x}) (\frac{\gamma(p, x/2)}{\Gamma(p)})^\eta \cdot dx \quad (10)$$

This expression can be solved in a piece-wise numerical manner. For single symbol accumulation, a simpler expression can be utilized for cell detection rates as shown in eqn. 11. These two expressions are utilized to compare cell search performance in the next sections.

$$P_d(snr, 1, \eta) = \int_0^\infty \frac{1}{2} e^{-\frac{(x+\lambda)}{2}} I_0(\sqrt{\lambda x}) (1 - e^{-\frac{x}{2}})^\eta \cdot dx \quad (11)$$

IV. System Architecture

Based on the design ideas presented earlier, an overall primary synchronization system architecture can be developed as shown in Figure 3. The analog RF component performs the frontend functionality of low-noise amplification (LNA), automatic gain correction (AGC), channel select (CS) filtering and analog to digital conversion (ADC). For the purposes of primary synchronization utilizing the PSS, both the in-phase and quadrature (I/Q) branches need a low pass filtering matching the bandwidth of PSS signal so as to eliminate the impact of higher sub-carriers as well as inherent thermal and white noise in the spectrum beyond the bandwidth of PSS signal. The I/Q samples supplied to PSS subsystem can be sampled at maximum rate of 30.72 Msps as per the 3GPP specifications. Based on this, a suitable sample timing hypothesis (H) and downsampling rate (R) needs to be utilized that reduces the number of parallel hypothesis to be evaluated as discussed in section III-A. For 30.72 Msps rate, the possible sample timing locations are $H = 153600$ (Table II). For first-stage coarse search procedure, an aggressive downsampling rate, $R = 16$ could be utilized. The OFDMA symbol duration (S) for a PSS symbol is 2048 samples, which results in the requirements of simultaneous evaluation of $\frac{S}{R}$ possible hypotheses. If clock source for PSS correlator is kept at symbol rate, because of downsampling, R parallel correlations can be performed for each timing hypothesis. This results in $\frac{S}{R^2}$ correlator units only. As an example, for 2048 sample PSS symbol duration, a downsampling rate of 16, only 8 correlator units will be needed in each of the I and Q branches. Once a coarse timing is known within $\pm\frac{R}{2}$ sample accuracy, a fine search at sample rate can be employed to determine the exact PSS symbol timing. This design employs storage of only $\frac{S}{R}$ time-domain PSS samples in ASIC itself for correlation purposes. These samples can be used as such during coarse search stage and will need to be resampled R-times for performing correlations at fine search stage. The correlated samples from each of I/Q branches need to be combined and accumulated. Also, three instances of PSS correlation stages need to be implemented in accordance with three possible values of roots of Zadoff-Chu sequence employed in PSS. The accumulated values need to be sorted in some useful manner to deliver the timing location with largest correlation magnitude. If only coherent combining is used and few top hypotheses are needed, this sorting operation can be done in real-time with no requirement for storing and accumulating correlated values. On the other hand, a non-coherent integration necessitates storage of accumulated values. The host processor can coordinate all the primary synchronization activities by means of interfacing control registers and procure results from the result registers. The key

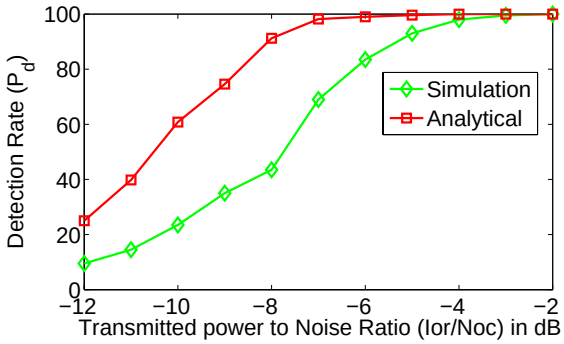

Fig. 4. Comparison of detection rates using analysis and simulations

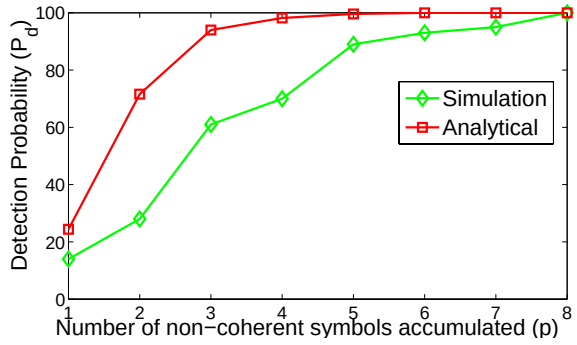

Fig. 5. Relation of cell detection rates on non-coherent accumulation for I_{or}/N_{oc} =-12 dB

for such a design lies in choosing appropriate downsampling rates R and choice of coherent vs. non-coherent accumulation that needs to be derived from system requirement for detection accuracy, available ASIC gate count and speed of cell search.

V. Design Results

An important metric in evaluating the performance of cell search procedure is the detection rate of cells with varying levels of signal to noise ratios. Figure 4 shows the achieved detection rates derived using analytical results as detailed in previous sections and simulations performed in ModelSim [12]. As anticipated the detection rate of a cell decreases with increasing levels of noise. The analytical results presented before provide a close approximation to actual simulation results. In general, the closed-form analytical results differ by around 2 dB from simulation results due to reasons such as non-zero correlations of PSS sequences at positions other than central peak position. The impact of noise induced on missed detections can be mitigated by non-coherent accumulations over multiple slots. Figure 5 shows the plot for detection rates improvements with increasing the number of non-coherent integrations. As is evident, for a worst-case scenario with $\frac{I_{or}}{N_{oc}}$ = -12 dB, the primary synchronization detection can be guaranteed to be nearly 100% by utilizing an 8-slot non-coherent integration. Based on these design ideals, a sample implementation was done utilizing *Altera*'s[13] Quartus II web edition and the gate count for the implementation are shown in table III. Overall, such a design is the culmination of design efforts based on sensitivity requirements and cell search speed. This can be ported to a system-on-chip design for a LTE modem for any hand-held device or data card.

TABLE III
Gate counts in FPGA implementation

Design Block	Gate Count
Correlator/Multiplier	4122
Shift Register	6144
Sample/PSS MUX	1404
Accumulator	1002
Sorter	2262

VI. Conclusion

In this paper, we have shown ideas for implementing a fast, efficient primary search procedure for the LTE systems. By means of analysis, relations have been derived for cell detection rates with varying levels of noise, number of non-coherently integrated symbols, and search granularity. Also, an exhaustive discussion has been presented that details the practical considerations in implementing a searcher block in ASIC based on these ideas. Finally, the analytical results are compared with simulations and generic performance trends are illustrated and benchmarked. As a future work, we intend to expand the model to include other design considerations such as inherent crystal frequency errors and fading phenomena in evaluating the searcher performance.

References

[1] A. Ghosh, J. Zhang, J. G. Andrews, R. Muhamed, "Fundamentals of LTE" *Prentice Hall* August 2010, ISBN:9780137033638.
[2] J. G. Proakis, D. K. Manolakis, "Digital Signal Processing", 4th ed., Prentice Hall, Apr. 2006.
[3] 3rd Generation Partnership Project, 3GPP TS 36.211, 36.521 March 2010, *ftp://ftp.3gpp.org/Specs/2011-06/Rel-10/36_series/*.
[4] Y. Tsai, G.Zhang, D. Grieco, F. Ozluturk, "Cell Search in 3GPP Long Term Evolution Systems" IEEE Vehicular technology Magazine, vol. 2, no. 2, pp.23-29, June 2007.
[5] K. Manolakis, G. Estevez, V. Jungnickel, W. Xu; C. Drewes, "A Closed Concept for Synchronization and Cell Search in 3GPP LTE Systems," Wireless Communications and Networking Conference, 2009. WCNC 2009. IEEE , vol., no., pp.1-6, 5-8 April 2009.
[6] C. -P. Li, W. -C. Huang; "A Constructive Representation for the Fourier Dual of the ZadoffChu Sequences", IEEE Transactions on Information Theory, vol. 53 , no. 11, pp. 4221-4224, 2007.
[7] P. -K.Tseng, S. H.Wang, C. P. Li, "A novel low complexity cell search scheme for LTE systems," Vechicular Technology Conference, 2010. VTC 2010-Spring. IEEE, pp.1-5, 16-19 May 2010.
[8] B. Lindoff, T. Ryden, D. Astley, "A robust cell search algorithm for 3GPP LTE", European Wireless Conference, 2009, EW 2009, pp. 303-307, 17-20 May 2009.
[9] L. .C. Wung, Y. C. Lin, Y. J. Fan, S. L. Su, "A robust scheme in downlink synchronization and initial cell search for 3GPP LTE system", Wireless and Pervasive Computing, 2011. ISWPC 2011, pp. 1-6, Feb 23-25, 2011.
[10] P.Y.Tsai, H.W.Chang, "A new cell search scheme in 3GPP long term evolution downlink, OFDM systems", Wireless Communications and Signal Processing IEEE, WCSP 2009, pp. 1-5, Nov 13-15, 2009.
[11] Technical Report, "Initial Synnchronization", Instt. of Comm. Engg., Nat. Sun Yat-Sen Univ., *http://140.117.160.140/CommEduImp/pdfdownload/9411/20051225/WCDMA-08-CellSearch.pdf*
[12] ModelSim, "Advanced Simulation and Debugging", *http://www.altera.com/products/software/quartus-ii/modelsim/qts-modelsim-index.html*
[13] Altera Quartus II web edition, *http://www.altera.com/products/software/quartus-ii/web-edition/qts-we-index.html*
[14] MATLAB, The Language of Technical Computing, v. 7.10, Mar. 5, 2010, MathWorks. *http://www.mathworks.com/products/matlab/*